

*Full Paper*

## **Electrochemical Behavior Assessment of Zircaloy-4 in Nitric Acid Solutions by Electrochemical Impedance Spectroscopy and Mott–Schottky Analyses**

**Arash Fattah-alhosseini\* and Marziyeh Nabaee**

*Department of Materials Engineering, Bu-Ali Sina University, Hamedan 65178-38695, Iran*

\*Corresponding Author, Tel.: +988138292505; Fax: +98 813 8257400

E-Mail: [a.fattah@basu.ac.ir](mailto:a.fattah@basu.ac.ir)

*Received: 5 October 2016 / Received in revised form: 22 November 2016 /*

*Accepted: 26 November 2016 / Published online: 15 February 2017*

---

**Abstract-** Zircaloy-4, one of zirconium alloys, has outstanding corrosion resistance to nitric acid. Utilizing potentiodynamic polarization, electrochemical impedance spectroscopy (EIS), and Mott–Schottky analyses, the electrochemical behavior of zircaloy-4 in nitric acid solutions were evaluated under open circuit potential (OCP) condition. At first, where the concentration of nitric acid increased from 0.01 to 0.05 M, the corrosion current density decreased. However, it amplified rapidly while the concentration increased from 0.05 to 0.50 M. Moreover, the EIS studies demonstrated an inverse trend for polarization resistance values. Mott–Schottky analysis indicated that the passive films displayed p-type semiconductive characteristics. Also, this analysis showed that the acceptor densities decreases by increasing nitric acid concentration from 0.01 to 0.05 M, whereas it increases when the nitric acid concentration reaches from 0.05 to 0.50 M. This trend was consistent resulting in potentiodynamic polarization and EIS measurements.

**Keywords-** Zircaloy-4, Nitric acid, Polarization, EIS, Mott–Schottky analysis

---

### **1. INTRODUCTION**

The outstanding corrosion resistance of zirconium and its alloys (especially zircaloy-4) in nitric acid and hydrochloric acid solutions has been known for over 60 years [1]. The previous studies [1–6] have revealed this metal and its alloys are highly resistant to nitric acid

solutions. In practice, zirconium and its alloys are extensively considered as candidate materials for the manufacturing various components such as dissolvers, oxalic mother liquor evaporator and heat exchangers [2–6].

Practically, the corrosion behavior of pure titanium improves as the impurity levels in hot nitric acid solutions increase. Titanium shows excellent corrosion resistance to recirculating nitric acid process streams. However, in hot and pure nitric acid solutions and vapor condensates of nitric acid, significant corrosion was seen for this metal [1]. Unlike titanium, zirconium and its alloys are unaffected by vapor condensates in boiling nitric acid. Zirconium and its alloys are much more corrosion resistant to nitric acid than titanium, but its susceptibility to stress corrosion cracking and corrosion fatigue are the only worries to the application of zirconium and its alloys [7,8].

Zirconium and its alloys are used in various industries due to the unique combination of properties like good ductility, strength and corrosion resistance in high temperature water. Controlled additions of tin, iron and chromium to zircaloy-2 lead to zircaloy-4, which has good corrosion resistance [1].

Although many studies have been published on the corrosion resistance of zirconium and its alloys [9–15], there is still lack of knowledge regarding the effect of nitric acid concentration on electrochemical behavior of zircaloy-4. Indeed, based on a literature survey, no previous work has been reported on the semiconducting behavior of zircaloy-4 in acidic solutions. The present research, to the best of our knowledge, is the first in its field focusing the effect of nitric acid concentration on electrochemical and semiconducting behavior of zircaloy-4. Therefore, potentiodynamic polarization, EIS and Mott–Schottky measurements of zircaloy-4 in nitric acid solutions of various concentration ranging from 0.01 to 0.50 M have been carried out in this work. It must be mentioned that the Mott–Schottky analysis is an important in-situ method for investigating the semiconductor properties [4,5,15].

## 2. EXPERIMENTAL PROCEDURES

Chemical composition of zircaloy-4 used in present investigation is shown in Table 1. It is supposed to explain that the alloy chemical composition was obtained by means of inductively coupled plasma optical emission spectrometry (ICP-OES). The structure of this alloy was analysed using the X-ray diffraction (XRD: Philips PW-1800) with Cu  $K_{\alpha}$  radiation ( $\lambda=0.1506$  nm). All Specimens were ground to P2000 (FEPA Standard) grit and cleaned with deionized water prior to testing. Aerated acidic solutions (without purging oxygen or any gas) with five different concentrations were used and the compositions were, respectively 0.01, 0.05, 0.10, 0.30 and 0.50 M  $HNO_3$ . All solutions were made from analytical grade 67%  $HNO_3$  and distilled water. The tests were carried out at  $25\pm 1$  °C. The detailed procedure of three-electrode flat cell was published elsewhere [15]. Prior to all electrochemical measurements, specimens were immersed at OCP condition for 2000 s to form a steady-state

condition. The potentiodynamic polarization curves were measured at a scan rate of 1 mV/s starting from  $-0.25 \text{ V}_{\text{Ag}/\text{AgCl}}$  (vs.  $E_{\text{corr}}$ ) to  $1.4 \text{ V}_{\text{Ag}/\text{AgCl}}$ . EIS tests were done at OCP condition and AC potential with the amplitude of 10 mV and a normal frequency range of 100 kHz to 10 mHz. Also, Mott-Schottky analysis was carried out at the frequency of 1 kHz using a 10 mV AC signal and a step potential of 25 mV, in the cathodic direction [15].

**Table 1.** Chemical compositions of zircaloy-4

Elements	Sn	Fe	O	Cr	Zr
Zircaloy-4 /wt%	1.35±0.01	0.21±0.01	0.11±0.002	0.09±0.001	Bal.

### 3. RESULTS AND DISCUSSION

#### 3.1. XRD evaluation

Fig. 1 shows zircaloy-4 XRD pattern. As demonstrated in Fig. 1, the strongest XRD diffraction peaks of zircaloy-4 are related to Zr and  $\text{Zr}_3\text{O}$ . Also, two peaks of SnO are seen, but the intensity of these peaks is weak. The XRD peak positions of an as-received sample is in very good agreement with the data for zircaloy-4 [16].

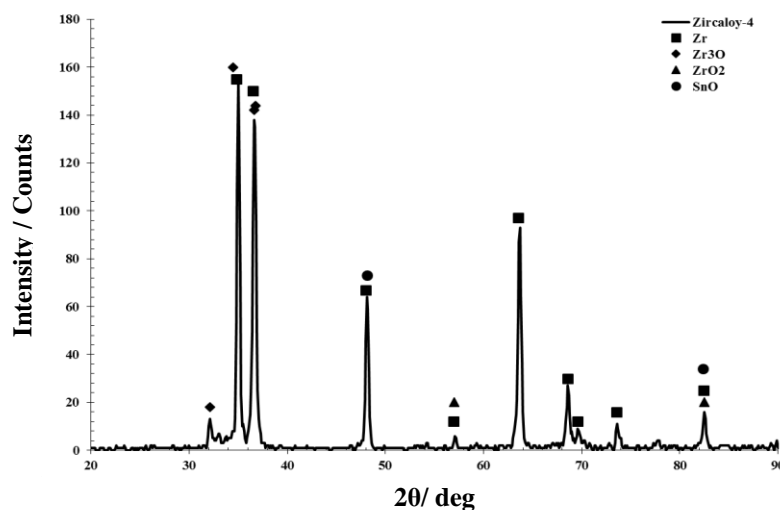


**Fig. 1.** XRD pattern of zircaloy-4

#### 3.2. Polarization measurement

Fig. 2 shows the potentiodynamic polarization curve of zircaloy-4 in nitric acid solutions. The current density was found to increase with potential during the early stage of passivation, and no current peak was observed. Also, it was seen that the passive potential range is

extending from the corrosion potential to  $1.4 \text{ V}_{\text{Ag}/\text{AgCl}}$ . Similar potentiodynamic polarization curve of zircaloy-4 in  $1.0 \text{ M HNO}_3$  solution have been shown by Priya et al. [17].

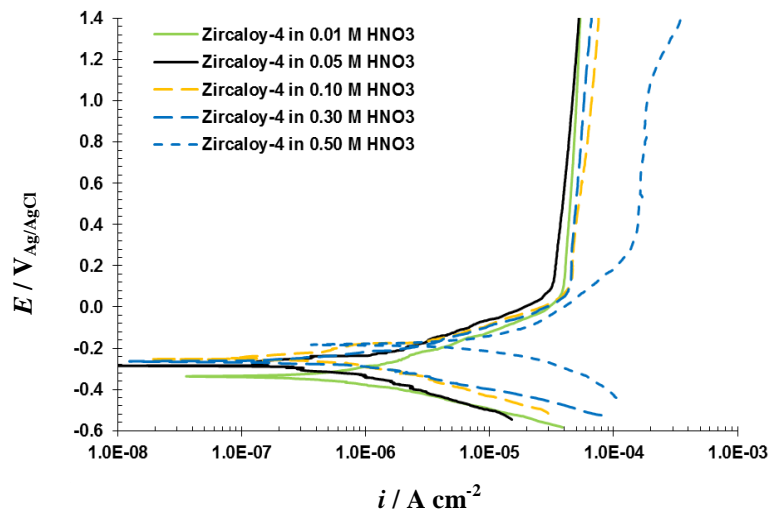


**Fig. 2.** Polarization curve of zircaloy-4 in nitric acid solutions

Fig. 3 demonstrates the values of the corrosion current density ( $i_{\text{corr}}$ ) versus the nitric acid concentration. It was observed that the corrosion current density of this alloy decreases by increasing nitric acid concentration from 0.01 to 0.05 M, while it increases when the nitric acid concentration reaches 0.50 M.

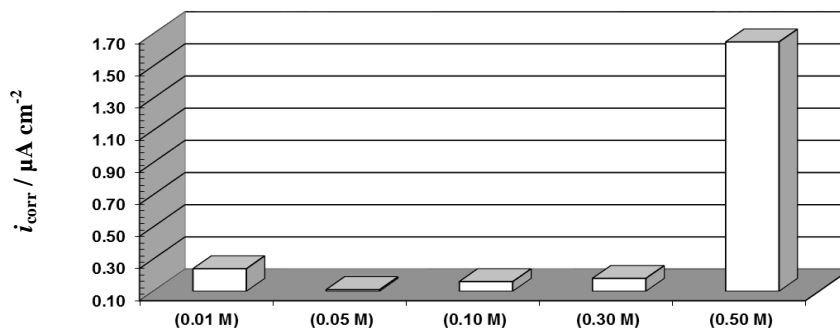


**Fig. 3.** Dependence of the corrosion current density on the nitric acid concentration

### 3.3. EIS measurements

The EIS response of zircaloy-4 in nitric acid solutions was determined, and the results were presented as Nyquist, Bode and Bode-phase plots in Fig. 4. All Nyquist plots show two imperfect semicircles. Also, the Bode and Bode-phase curves show two constant times. Similar Nyquist plots for ZrTi alloys in aerated Ringer's solution have been reported by Bolat et al. [12].

Based on the Nyquist and Bode plots, the equivalent circuit shown in Fig. 5 (with two time constants) was used to simulate the measured impedance data of zircaloy-4. This equivalent circuit have been used successfully by Goossens et al to simulate the zirconium oxide measured impedance data in 1 M  $\text{H}_3\text{PO}_4$  solution [18]. In this equivalent model,  $Q_p$  is the constant phase element of the passive film,  $R_p$  is the passive film resistance,  $Q_{dl}$  is the constant phase element of the double layer,  $R_{ct}$  is the charge-transfer resistance, and  $R_s$  represents the solution resistance. It is clear that the passive metal corrosion is hindered by an oxide film that acts as a barrier-type compact layer.

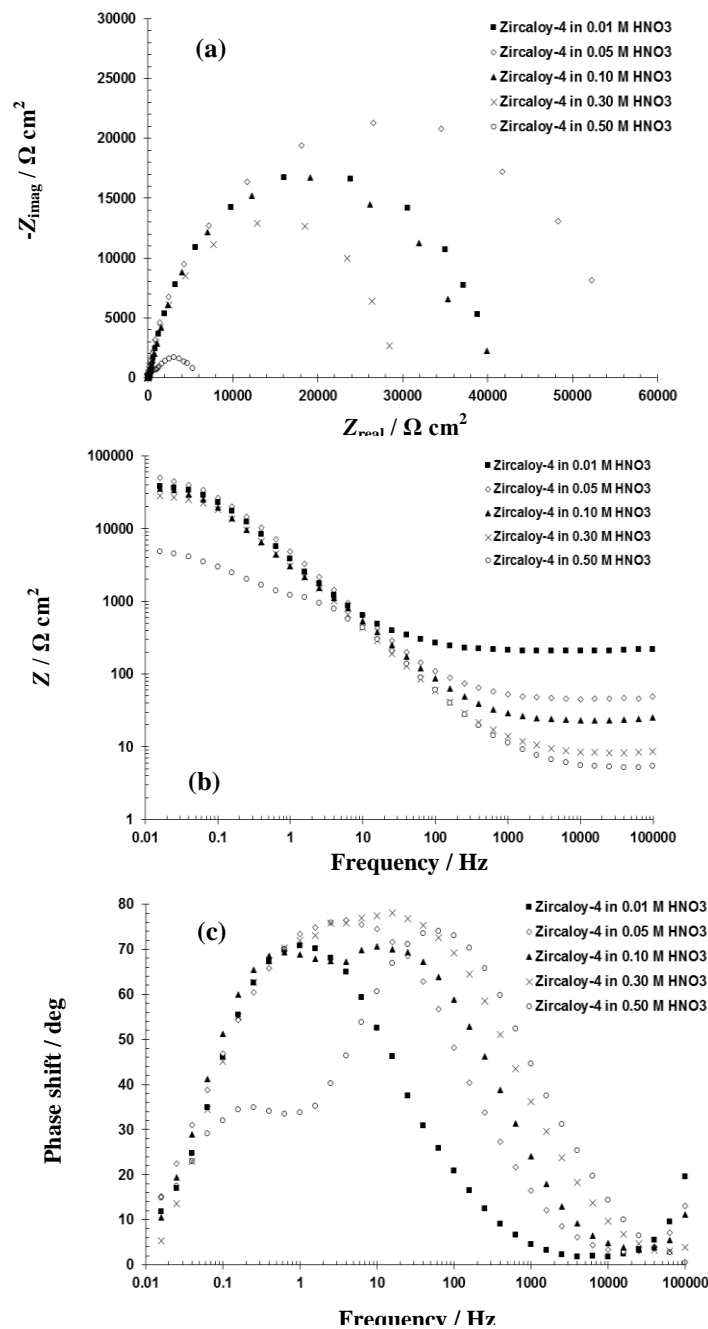


**Fig. 4.** (a) Nyquist, (b) Bode, and (c) Bode-phase plots of zircaloy-4 in nitric acid solutions

It is necessary to mention that the impedance of the constant phase element is presented using Eq. (1) [19–22]:

$$Z_Q = [C(j\omega)^n]^{-1} \quad (1)$$

In Eq. (1),  $n$  is associated with the roughness of the electrode surface.

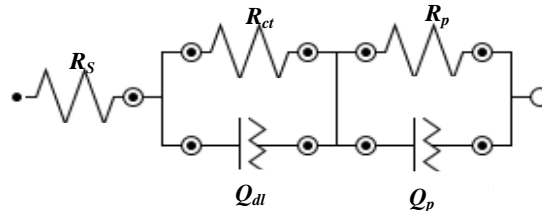


**Fig. 5.** The best equivalent circuit tested to model the experimental EIS data [18]

Fig. 6 illustrates the effect of nitric acid concentration on polarization resistance ( $=R_p+R_{ct}$  [23]) of zircaloy-4. At first, where the concentration of nitric acid increased from 0.01 to 0.05 M, the polarization resistance increased. However, it decreased rapidly while the concentration increasing from 0.05 to 0.50 M.

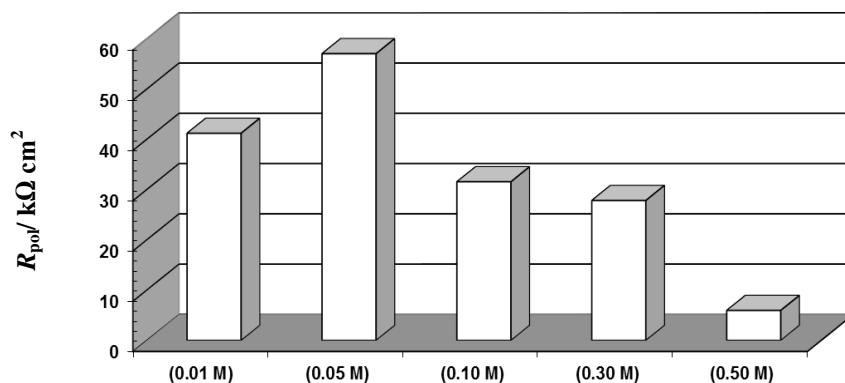


**Fig. 6.** Dependence of the polarization resistance on the nitric acid concentration

### 3.4. Mott–Schottky analysis

Fig. 7 shows the Mott–Schottky plots of zircaloy-4 in nitric acid solutions.

As can be seen, clear  $C^{-2}$  clearly decreased as nitric acid concentration increased. In this figure, the negative slopes are attributed to p-type behavior. However, recently the Mott–Schottky plots with n-type behavior for zirconium in alkaline solution (0.5 M NaOH, pH=13.3) have been reported [15].

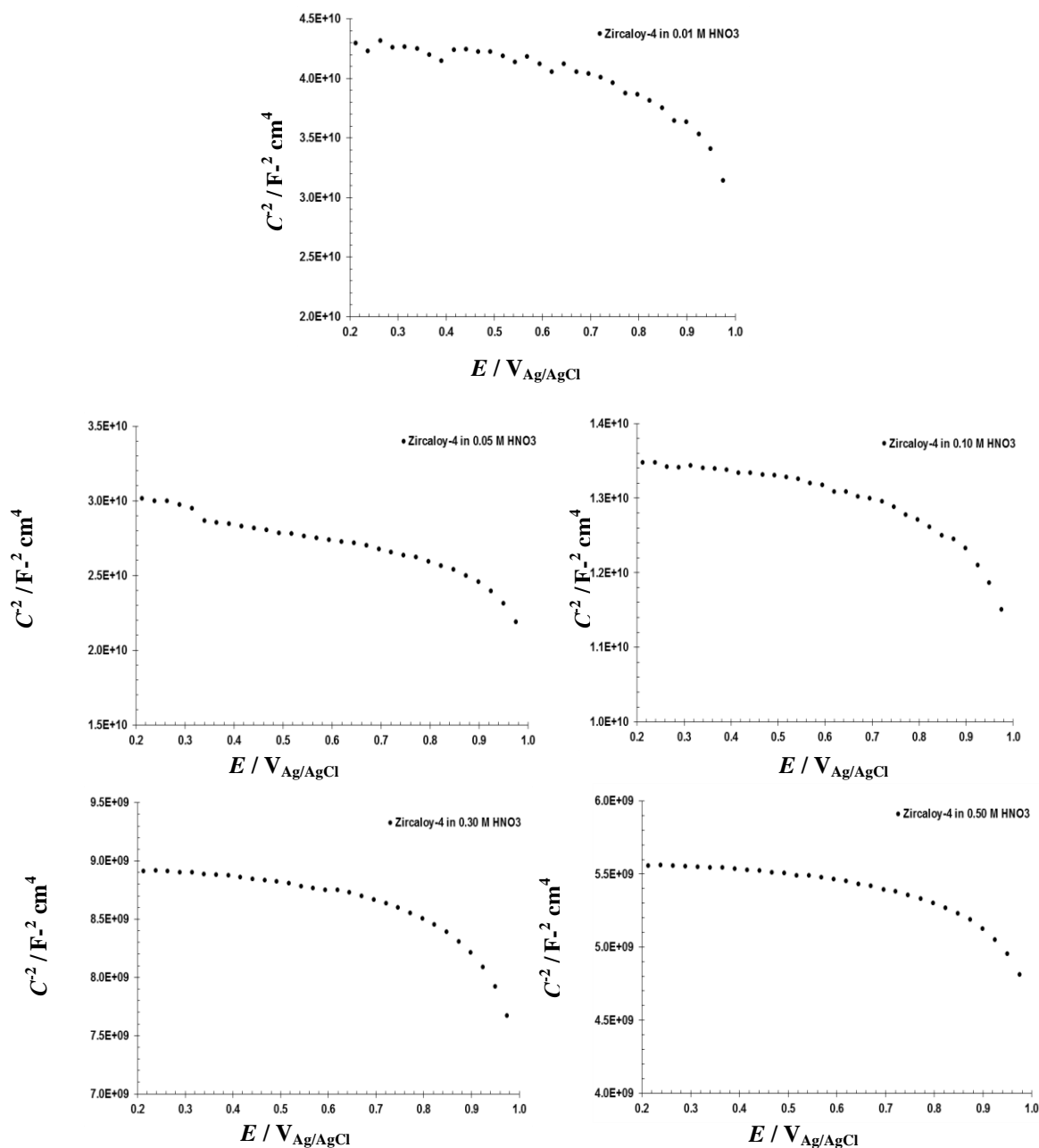


**Fig. 7.** Mott-Schottky plots of zircaloy-4 in nitric acid solutions

The acceptor density of the passive film formed on zircaloy-4 nitric acid solutions was determined from these negative slopes according to Eq. (3) [2,22-24]:

$$\frac{1}{C_{SC}^2} = -\frac{2}{\varepsilon \varepsilon_0 e N_A} \left( E - E_{FB} - \frac{k_B T}{q} \right) \quad (3)$$

In this equation:  $\varepsilon$  is the dielectric constant of the passive film ( $\varepsilon=22$  for zirconium and its alloys [2,15]),  $\varepsilon_0$  is the vacuum permittivity ( $8.854 \times 10^{-14}$  F/cm),  $e$  is the electron charge,  $N_A$  represents the acceptor density for  $p$ -type semiconductors ( $\text{cm}^{-3}$ ),  $k_B$ ,  $T$ , and  $E_{FB}$  are the

Boltzmann constant, absolute temperature, and flat band potential, respectively [2,15]. Fig. 8 shows the effect of nitric acid concentration on the calculated acceptor density of the passive film formed on zircaloy-4.

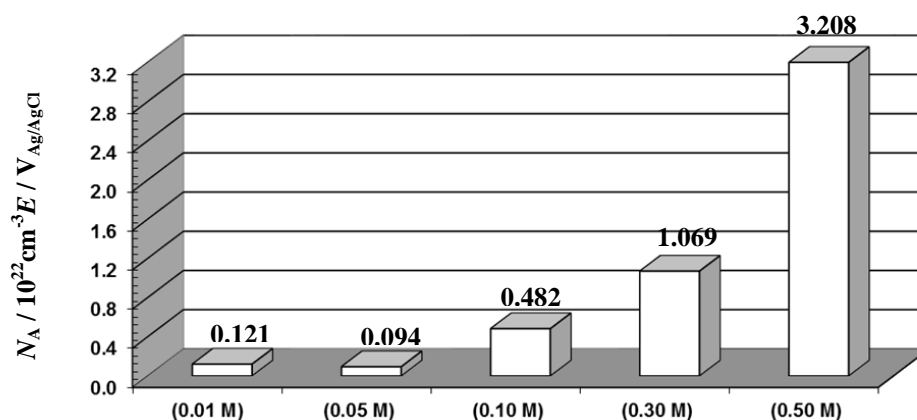


**Fig. 8.** Acceptor densities of the passive films formed on zircaloy-4 in nitric acid solutions

As can be seen, the order of magnitudes are around  $10^{22} \text{ cm}^{-3}$ . At first, the acceptor density decreases by increasing nitric acid concentration from 0.01 to 0.05 M, while it increases when the nitric acid concentration reaches 0.50 M. This trend was consistent with the results of the potentiodynamic polarization (variation of the corrosion current density (Fig. 3) and EIS measurements (variation of the polarization resistance (Fig. 6)).

To investigate the effect of nitric acid concentration on the passive film growth, we can use the point defect model. Using this model, we can obtain the analytical expression for the concentration of vacancies within the passive film. This model shows the cation vacancies are electron acceptors (p-type semiconductor), whereas the oxygen vacancies and the metal interstitials are electron donors (n-type semiconductor) [23,24]. According to Fig. 8, the high values of the acceptor density are attributed to a higher density of the zirconium vacancies ( $\text{Zr}^{4+}$  vacancies) in the passive films. Indeed, increasing nitric acid concentration from 0.05 to 0.50 M give worse conditions for forming the passive films with lower protection behavior, due to the growth of a higher defective passive film.

#### 4. CONCLUSIONS

In this work, the electrochemical behavior of zircaloy-4 in nitric acid solutions has been explored using potentiodynamic polarization, EIS, and Mott–Schottky analyses. The principal findings and conclusions of this work are as follows:

1. Potentiodynamic polarization curves demonstrated that zircaloy-4 showed good passive behavior in nitric acid solutions. Moreover, these curves showed that the corrosion current density decreased by increasing the concentration of nitric acid from 0.01 to 0.05 M. however, it amplified rapidly as the concentration increased from 0.05 to 0.50 M.

2. The EIS data showed that the polarization resistance increased by increasing the concentration of nitric acid from 0.01 to 0.05 M, however, it decreased rapidly as the concentration increased from 0.05 to 0.50 M.
3. The experimental data of Mott–Schottky analysis was interpreted in terms of the point defect model for the passivity of zircaloy-4 in nitric acid solutions, assuming that the acceptors were defects including zirconium vacancies. Also, based on this analysis, it was shown that the acceptor densities decreases by increasing nitric acid concentration from 0.01 to 0.05 M, while it increases when the nitric acid concentration reaches from 0.05 to 0.50 M.
4. The results of potentiodynamic polarization, EIS and Mott–Schottky analysis showed that increasing nitric acid concentration from 0.05 to 0.50 M give worse conditions for forming the passive films with lower protection behavior, due to the growth of a higher defective passive film.

## REFERENCES

- [1] A. Ravi Shankar, V. R. Raju, M. Narayana Rao, U. Kamachi Mudali, H. S. Khatak, and B. Raj, *Corros. Sci.* 49 (2007) 3527.
- [2] Y. Chen, M. Urquidi-Macdonald, and D. D. Macdonald, *J. Nucl. Mater.* 348 (2006) 133.
- [3] S. J. Lee, E. A. Cho, S. J. Ahn, and H. S. Kwon, *Electrochim. Acta* 46 (2001) 2605.
- [4] V. D. Jovic', and B. M. Jovic', *J. Electrochem. Soc.* 155 (2008) C183.
- [5] V. D. Jovic', and B. M. Jovic', *Corros. Sci.* 50 (2008) 3063.
- [6] Y. Choi, J. W. Lee, Y. W. Lee, and S. I. Hong, *J. Nucl. Mater.* 256 (1998) 124.
- [7] T. Motooka, and K. Kiuchi, *Corrosion* 8 (2002) 703.
- [8] B. Raj, and U. Kamachi Mudali, *Prog. Nucl. Energy* 48 (2006) 283.
- [9] Y. Tsutsumi, Y. Takano, H. Doi, K. Noda, and T. Hanawa, *Mater. Sci. Forum* 561-565 (2007) 1489.
- [10] J. Ai, Y. Chen, M. Urquidi-Macdonald, and D. D. Macdonald, *J. Nucl. Mater.* 379 (2008) 162.
- [11] B. Kim, C. Park, and H. Kwon, *J. Electroanal. Chem.* 576 (2005) 269.
- [12] G. Bolat, J. Izquierdo, D. Mareci, D. Sutiman, and R. M. Souto, *Electrochim. Acta* 106 (2013) 432.
- [13] M. Santamaria, F. D. Quarto, and H. Habazaki, *Electrochim. Acta* 53 (2008) 2272.
- [14] T. Hurlen, and S. Hornkj, *Electrochim. Acta* 32 (1987) 811.
- [15] A. Fattah-alhosseini, and N. Attarzadeh, *Anal. Bioanal. Electrochem.* 7 (2015) 254.
- [16] A. Pshenichnikov, J. Stuckert, and M. Walter, *Nucl. Eng. Design* 283 (2015) 33.
- [17] R. Priya, C. Mallika, and U. Kamachi Mudali, *Wear* 310 (2014) 90.
- [18] A. Goossens, M. Vazquez, and D. D. Macdonald, *Electrochim. Acta* 41 (1996) 47.

- [19] F. Y. Zhou, B.L. Wang, K. J. Qiu, W.J. Lin, L. Li, Y. B. Wang, F. L. Nie, and Y. F. Zheng, *Mater. Sci. Eng. C* 32 (2012) 851.
- [20] C. H. Huang, J.C. Huang, J. B. Li, and J. S. C. Jang, *Mater. Sci. Eng. C* 33 (2013) 4183.
- [21] F. Rosalbino, D. Maccio, A. Saccone, E. Angelini, and S. Delfino, *Mater. Corrosion* 63 (2012) 580.
- [22] S. O. Gashti, and A. Fattah-alhosseini, *Anal. Bioanal. Electrochem.* 6 (2014) 535.
- [23] A. Fattah-alhosseini, *Arab. J. Chem.* DOI:10.1016/j.arabjc.2012.02.015.
- [24] A. Fattah-alhosseini, and S. Vafaeian, *Appl. Surf. Sci.* 360 (2016) 921.